Supplementary Information

Plasmon Mediated Shape and Size Selective Synthesis of Icosahedral Silver Nanoparticles via Oxidative Etching and Their 1-D Transformation to Pentagonal Pins

by Rachel Keunen, Nicole Cathcart, Vladimir Kitaev

Effect of Copper and Other Metal Dopants

In order to elucidate the role of copper in the system, we have tested the effect of several other metal ions (Pd(II) (**Fig. S7A**), Fe(III) (**Fig. S7B**), and Co(II) (**Fig. S7D**)) that could possibly function similarly in the formation of AgI_hNPs. Generally, we were not able to find conditions where different metals ions worked the same as copper cations. Upon using similar concentrations (0.15 mM – 1.2 mM) of cobalt(II) perchlorate instead of Cu^{2+}, the resulting AgNPs featured a significant fraction of large platelets and very few AgI_hNPs (**Fig. S7D**). Similarly, addition of iron(III) perchlorate instead of Cu^{2+} led to the formation of different polyhedral AgNPs, as well as the formation of an iron oxide shell around AgNPs, as can be seen in **Fig. S7B**. When Cu^{2+} was *replaced by* Pd(II) (2 μM Pd(II), 33:1 Ag:Pd molar ratio). A noticeably higher fraction of misshapen nanoparticles and platelets formed in addition to a very small number of AgI_hNPs (**Fig. S7A**). When palladium(II) acetylacetonate was used *in addition to* Cu^{2+} (2 μM Pd(II), 33:1 Ag:Pd molar ratio), AgI_hNPs still formed, however with a much higher proportion of small or misshaped AgI_hNPs (**Fig. S8A**). It is likely that less reactive palladium inhibits growth of icosahedral seeds into larger AgI_hNPs. The one metal that had successful results in conjunction with Cu^{2+} was cobalt. The AgI_hNPs synthesized using cobalt (II) chloride (1.82 μM Co(II), 36:1 Ag:Co molar ratio) were more nicely faceted than those synthesized with other metal dopants; however, there was a larger percentage of smaller MNPs present in the Co-doped samples (**Fig. S8B**) and further synthesis optimization is required to refine this system.

Effect of Light Exposure

Light intensity and exposure times were found to be not overly critical parameters (**Fig. S12**) and did not significantly affect the size-dispersity of the population or the shape selectivity in AgI_hNP formation. Typically, 3-6 ml of a precursor solution was exposed to 1 W LED (ca. 300 mW specified light output) for 17-24 hours (see Experimental). The onset of AgI_hNP formation could be detected by UV-vis spectroscopy as fast as 5 minutes after the start of light exposure (spectra ❷ in **Fig. S12**). Varying effective light exposure by using smaller precursor volumes and lower light intensities did not bring significant changes. These results are different compared to decahedra photochemical growth where using higher power of blue light (435-480 nm) was found to be beneficial.[1] A weaker dependence of AgI_hNP formation on the light power is likely due to the lower silver concentration in the system (0.05 mM compared to 0.12 mM for decahedra).[1]

Our first successful AgI_hNP synthesis employed a metal halide lamp with relatively uniform intensity throughout a visible range as the light source (❸ in **Fig. S20A**). The resulting AgNPs were predominantly icosahedral (40-60% shape yield, **Fig. S20B**) however it was difficult to avoid substantial impurities of decahedral and other less-defined AgNPs due to the wide spectral range of the light source that promoted formation of different morphologies.[2]

Effect of Oxidative Etchants

In addition to a very narrow optimal concentration range, the timing of the addition of hydrogen peroxide relative to the addition of the reducing agent, $NaBH_4$, is very important. The best results were achieved when the hydrogen peroxide was added within two minutes of the $NaBH_4$ addition and as close as possible to the start of the light exposure. Such timing of peroxide addition helps to limit the thermal growth of the seed particles that are not icosahedral. The reduction side in the red-ox equilibrium is first accomplished by sodium borohydride and then during the light exposure – by citrate. A constant presence of reducing agents during the AgI_hNP synthesis assures that most of the silver remains in the metallic form and prevents the formation of new seed particles that are not icosahedral.

Many different variations of amounts and timing for the addition of H_2O_2 have been tested due to the key role of etching in the AgI_hNP synthesis. One unsuccessful method of H_2O_2 addition was its continuous dispensing over a period of time between 15 minutes and 8 hours. Continuous addition of the same amounts of H_2O_2, that typically yielded a high fraction of AgI_hNPs when added in one portion, led to complete AgNP dissolution. On the other hand, a variation on this method, in which the hydrogen peroxide was added in several (typically two) portions at different points during the AgI_hNP growth, was most successful. Using the latter method we were able to largely eliminate smaller particles from the final AgI_hNPs.

To demonstrate a general validity of the use of oxidative etchants in AgI_hNP synthesis and to potentially improve on the etching, we have tested several peroxo-based etchants. Persulfate was another etchant that worked in the AgI_hNP synthesis both in conjunction with and replacing H_2O_2. Persulfate was capable of dissolving the AgNPs at much lower concentrations (ca. 10.8 mM) than the H_2O_2 (ca. 1.1 M in the absence of polymer) (**Fig. S5C**). The likely reason for higher persulfate effectiveness is the negative charge that enhances its interactions with silver ions both in solution and at the surface of AgNPs. Persulfate did work under the reaction conditions used for hydrogen peroxide only with a lower persulfate concentration of 10.8 mM (see Experimental). However, in several experimental series that we have performed, we could not achieve the same AgI_hNP shape selection as with H_2O_2. It is possible that different conditions may be found where persulfate or other peroxo- species will serve as effective shape-selective etchants.

The Role of Chloride in Oxidative Etching

The most effective chloride concentration in the system prior to the reduction was found to be ca. 18 μM corresponding to the molar ratio of silver to chloride of 375:1. Higher chloride concentrations (>0.18 μM) were detrimental for AgI_hNP synthesis due to the enhancement of AgNP dissolution via chloride strong binding to silver (silver redox potential is effectively lowered in the presence of chloride).

We also had some limited success with post-modification using halides, specifically when chloride ions (ca. 5-20 μM) were added to already prepared icosahedra for subsequent thermal treatments. The AgI_hNP shape-selection improved, albeit not very significantly, after such treatments (**Fig. S14**). These experiments also highlight a very good resistance of the prepared AgI_hNPs to prolonged heating and

light exposure, which can be attributed to high icosahedron symmetry and stability of its (111) surface facets in the presence of citrate.

Effect of Sterically Stabilizing Polymers

Overall, we have tested PVP, PSS, poly(4-vinylpyridine), and poly(acrylic acid) in the capacity of a sterically stabilized polymer in the system (**Fig. S6**) (see Experimental Methods). **Fig. S6F** shows a TEM image of an AgNP sample prepared using poly(4-vinylpyridine). It can be seen there that while AgI_hNPs do develop, the resulting particles are size-disperse with the significant presence of other morphologies. **Fig. S6G** shows a sample produced using a high molecular weight (450,000 g/mol) poly(acrylic acid). This sample does contain a large number of AgI_hNPs; however, the AgI_hNPs have high size-dispersity and large platelets are also present. **Fig. S6B,E** illustrates AgNPs synthesized using PVP. These AgNPs have a relatively high fraction of icosahedra; however, compared with the samples prepared using PSS (**Figs. S6C,D**) and no polymer (**Figs. 2, 3, S6A**), the size-selectivity of these AgI_hNPs is inferior. Upon comparison of sterically stabilizing polymers in the system, the best results have been obtained with PSS. Smaller PSS amounts (ca. 4.5:1 molar ratio of Ag to PSS) were found optimal for the size-selective AgI_hNP synthesis (**Figs**. **S6C,D**). The best samples containing PSS were found to have high size-selectivity amongst the population of larger AgI_hNPs but also noticeable amounts of smaller AgI_hNPs and less-defined particles (**Figs**. **S6C,D**). Eventually it was realized that the best size-selection of AgI_hNPs can be achieved without the use of sterically protecting polymers that tend to stabilize the smaller particles and hamper their dissolution by oxidative etching (**Figs. 2 & 3**).

Effect of Silver Concentration

Our first-generation AgI_hNP synthesis started with commonly used silver concentration of 0.1-0.15 mM.[3,4] Through the subsequent testing of different silver concentrations, the optimal range for AgI_hNP synthesis was found to be lower at ca. 65-80 μM. At higher silver concentrations, there is less shape-selectivity: noticeable formation of platelets becomes a major interfering process. At lower silver concentrations (<65 μM), AgNP dissolution starts to present noticeable problems, and also there is less silver to produce appreciable amounts of AgI_hNPs. Lower optimal silver concentrations in the AgI_hNP synthesis can be rationalized as being beneficial for the formation of the smallest stable nuclei, which are icosahedral.[5] In addition, lower silver concentration is advantageous for the uniform photochemical development due to better penetration of more scattered violet light.

Effect of Reducing Agents: $NaBH_4$, Ascorbic Acid, and Citrate

Sodium borohydride acts as a primary reducing agent in the AgI_hNP synthesis converting Ag^+ to metallic silver, while sodium citrate functions as a secondary reducing agent that is triggered photochemically.[6] Without the use of $NaBH_4$ the formation of AgNPs is not initiated. We have found that an optimal amount of $NaBH_4$ in the system is ca. 2.8 mM for the total concentration in solution. Such relatively high amounts of borohydride (>50:1 molar ratio to silver) are required to first completely convert all silver to a metallic form and then to counteract oxidative etching of AgNPs upon addition of peroxide. Higher borohydride concentrations (ca. 4.5 mM) lead to the prevalence of decahedral AgNPs in the sample. The formation of decahedra can be seen by the shoulder in the UV-vis spectrum at ca. 530 nm (❷ in **Fig.**

S21). When the concentration of sodium borohydride is lower than optimal (2.2 mM) the spectrum of resulting AgNPs become much broader that is indicative of high size-dispersity (❸ in **Fig. S21**).

In a series of experiments, we were able to demonstrate that sodium borohydride is not essential as the primary reducing agent for the AgI_hNP synthesis. Borohydride can be replaced by ascorbate. Despite that ascorbate is a milder reducing agent, concentrations similar to those used for borohydride (ca. 2.6 mM), worked the best. This can be due to the large excess of reducing agent typically used (ca. 50:1 molar to silver) and fast borohydride decomposition in neutral aqueous solutions. Under the screened conditions, AgI_hNPs prepared with ascorbate had appreciably broader size distribution and were less faceted (**Figs. S22A**,**B**). Further optimization of the synthesis with ascorbate is required to achieve better shape control in this system.

While sodium citrate can function as a reducing agent, it reacts very slowly with silver ions at room temperature. Upon light exposure citrate is photochemically activated at the surface of plasmonic AgNPs[6] and becomes instrumental for establishing the equilibrium between the reduction and oxidation of silver.

Citrate also has another important role as a charge-stabilizing agent. Citrate was shown to stabilize (111) Ag surfaces[4,6] and is essential for the formation of well-defined AgI_hNP facets. Very low citrate concentration in the system leads to ill-shaped aggregates (**Fig. S22C**). Due to a very narrow window of optimal etching conditions, there is also a narrow range of optimal citrate concentrations despite the significant excess of the citrate. Deviations of ca. 10% from the optimum concentration (which is dependent on peroxide concentration and the mode of peroxide addition) tend to cause an increase in the decahedral shoulder in the UV-vis spectra (❷ in **Fig. S23**). This shoulder at ca. 500-550 nm corresponds to larger decahedral AgNPs and starts to appear as the concentration of citrate is increased above ca. 1.7 mM in the samples containing tetrachloroaurate and sterically stabilizing polymers. At higher concentrations of hydrogen peroxide, the citrate concentration also has to be increased to maintain the red-ox equilibrium in the AgI_hNP synthesis.

Effect of pH in AgI_hNPs synthesis

Maintaining a slightly basic pH in the range from ca. 7.8 to 9.4 is essential for the formation of size- and shape-selected AgI_hNPs. The best results are achieved when the pH is not altered by the addition of either acid or base to the original preparation described in the Experimental Methods. Variation of pH was accomplished by replacement of citrate with citric acid and addition of KOH. Citrate is responsible for the basic pH of the system since it is a conjugate base of a weak citric acid with pK_a values of 3.14, 4.76, and 6.4. The effect of pH on formation of AgI_hNPs is summarized in **Fig. S24** where the spectra corresponding to samples prepared at weakly basic pH (≤9.4) feature peaks characteristic of AgI_hNP (❺-❼ in **Fig. S24)**. At an acidic pH (≤7), the spectra are indicative of small AgNPs, which become the main product with no AgI_hNPs present (spectrum ❾ in **Fig. S24**). At pH > 11, a diverse population of different morphologies is evident from the spectra (❶&❷ in **Fig. S24**) with only a small fraction of AgI_hNPs observed by EM.

Effect of Stirring Conditions in AgI_hNP synthesis

AgI_hNP formation is highly sensitive to subtle changes in synthetic conditions. Consequently, testing optimal conditions of stirring, such as spin speed and type of magnetic stir bar becomes important. Both of these parameters were found to have an appreciable effect on the delicate red-ox equilibrium of silver in the system. The best spin speed was determined to be moderate at ca. 90 rpm with a typical rod-shaped stir bar (12.7 mm by 3.2 mm) (**Figs. S25** & **S26**). Upon stirring speeds below 90 rpm or gentle shaking instead of stirring, the fraction of small or misshapen AgNPs increases greatly (❶ and ❺ in **Fig. S25**). Above 90 rpm, decahedral AgNPs tend to form, as shown by the larger decahedra shoulder at ca. 530 nm in spectrum ❹ of **Fig. S25**. A possible reason for the increase in the decahedral AgNPs is that upon intense stirring more collisions of precursor particles can take place so that the large cluster nuclei will be favored, specifically decahedral vs. icosahedral.

Similar trends are also observed for different types of stir bars, as shown in **Fig. S26**. Spectrum ❶ in **Fig. S26** (9.5 mm by 5.5 mm cross stir bar) is more characteristic of small AgI_hNPs or misshapen NPs than spectrum ❷ (12.7 mm by 3.2 mm cylindrical stir bar), though the difference is slight. However, spectrum ❸ in **Fig. S26** (15.9 mm by 9 mm large octagonal stir bar) has a large shoulder at ca. 500 nm indicative of the development of decahedra that is not observed in spectrum ❷. The monodispersity of AgI_hNPs prepared using a larger 9.5 mm cross stir bar is inferior, as can be seen from the comparison of **Fig. S26B** with **Figs. 2** and **3**. Given these observations, the 12.7 mm by 3.2 mm stir bar at ca. 90 rpm was determined to be optimal for the developed AgI_hNPs synthesis.

Gold Plating of AgI_hNPs

Testing the universality of the previously developed gold plating procedure,[7] we have prepared several gold-plated samples of AgI_hNPs that are stable in 0.2 M hydrogen peroxide and feature well preserved AgI_hNP integrity including the faceting (**Fig. S3A**). The optimal molar ratio of gold relative to silver for the plating was 20% – at the higher ratio of 80%, formation of AgI_hNP gold shells takes place (**Fig. S3B**). Preparation of thin gold frames using AgI_hNPs as a template has been demonstrated previously.[8]

Table S1. Summary of experimental conditions* of the synthesis of high-quality AgI_hNPs.

Citrate (mM)	Polymer (μM)	$HAuCl_4$ (μM)	KCl (μM)	$NaBH_4$ (mM)	H_2O_2 (M)	LED Maximum (nm)	AgI_hNP SPR Maximum (nm)	Corresponding Figure of EM Image
1.58	---	4.3	---	2.72	0.595	409	453 & 449	3b & 2b
1.60	---	4.3	---	2.76	0.604	409	447	3i
1.62	---	4.4	---	2.79	0.351	401	439	3c
1.60	---	---	0.018	2.77	0.348	409	421	2d
1.61	---	4.4	---	2.78	0.533	409	451	2e
1.95	---	0.72	14	2.75	0.286	409	425	2a
1.62	---	4.4	---	2.80	[a]0.291 +0.031	409	453	3e
1.62	---	0.74	15	2.79	0.260	409	425	S4A
1.63	---	---	---	2.81	0.654	409	421	2c
1.98	160[c]	---	---	3.37	0.297	409	435	S4C
1.96	14.5[c]	---	---	3.33	[b]0.407	401	427	S4D

* Total reaction volumes of 6.75 to 7.25 mL and total concentrations of 0.065 mM $AgNO_3$ and 0.29 mM $CuSO_4$, see Methods.

[a] Two portions 30 minutes apart.

[b] Hydrogen peroxide was added before sodium borohydride instead of the reverse.

[c] PSS

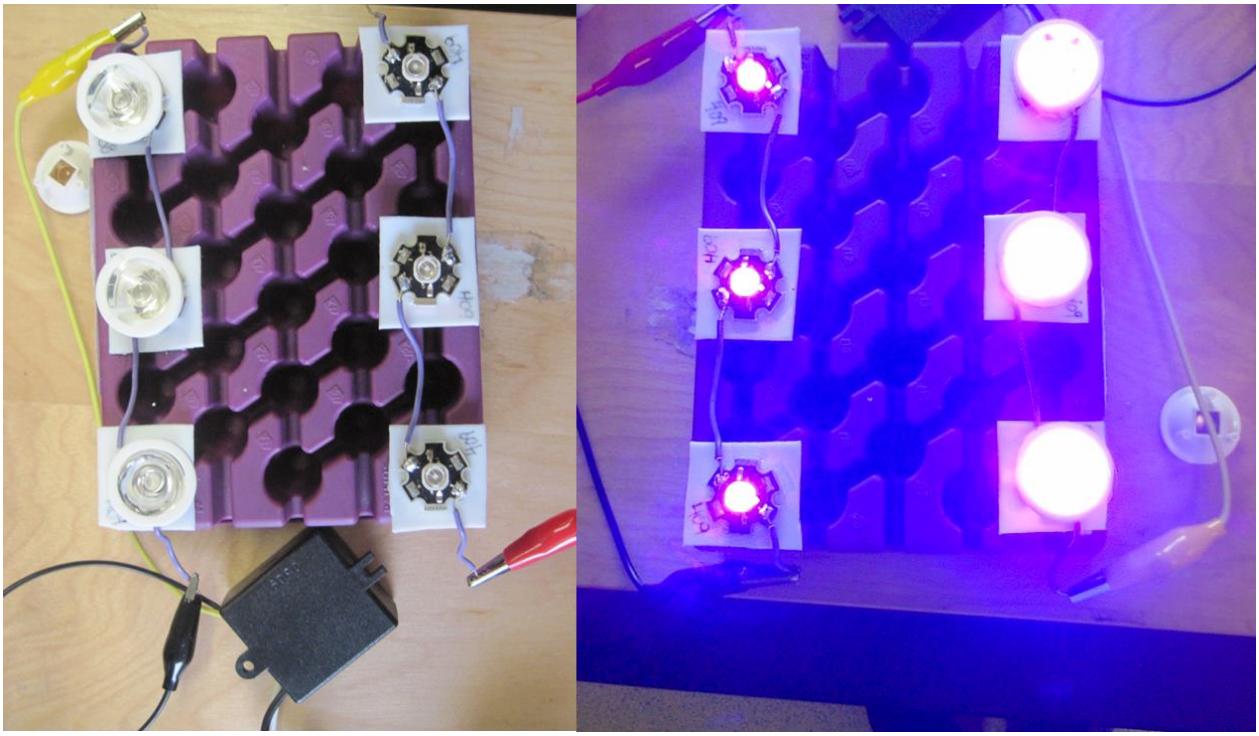

Figure S1. Photographs of the LED setup for light exposure of the AgI_hNP samples.

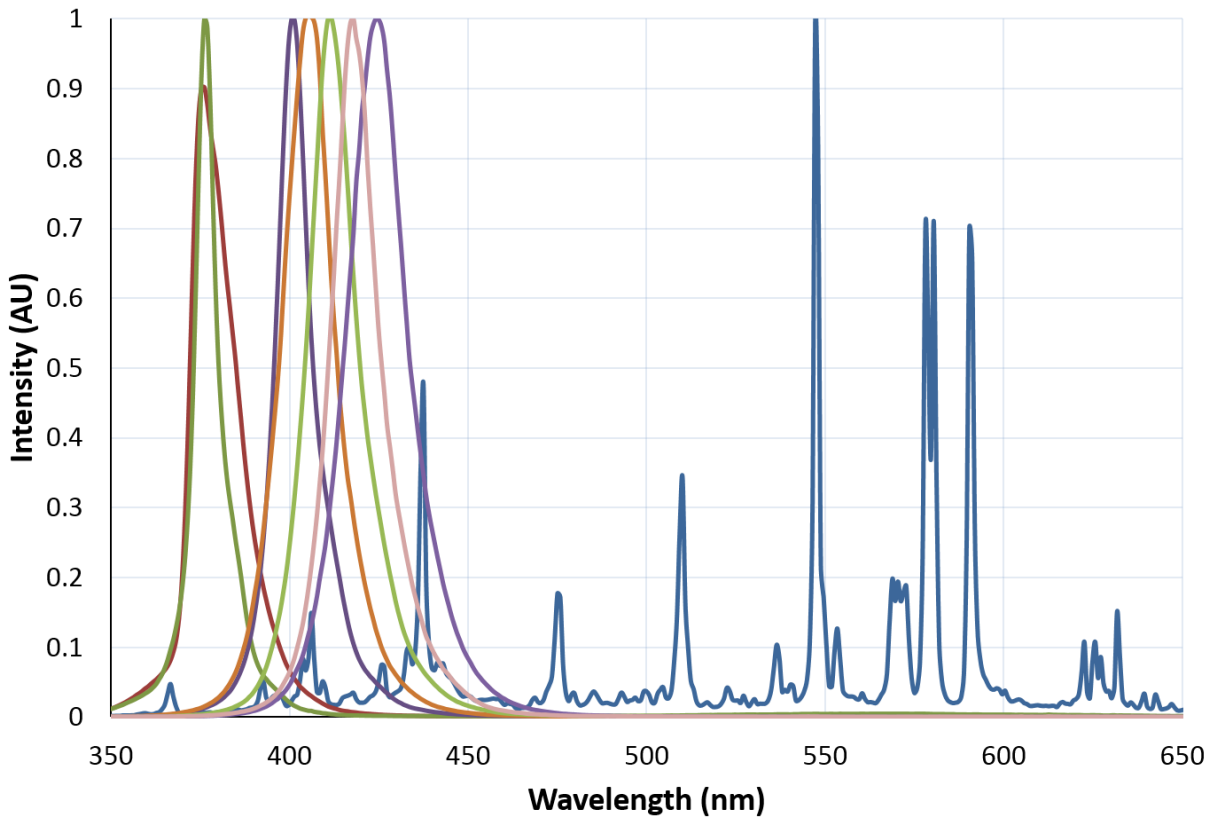

Figure S2. Emission spectra of the light sources used in the growth of the AgI_hNPs: LEDs (ranging from 375 nm to 435nm) and metal halide lamp (360-650 range).

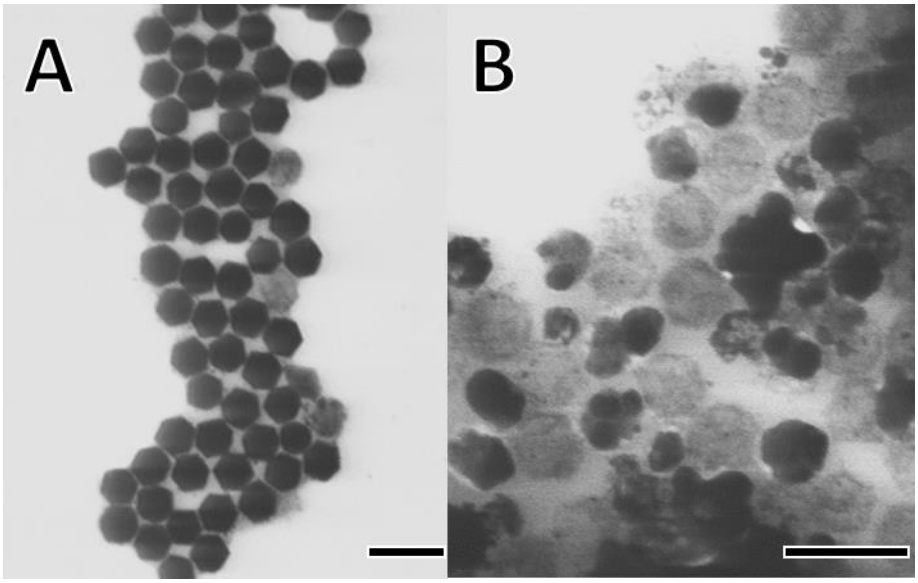

Figure S3. TEM images of gold modification of AgI_hNPs. **A)** Gold plating (20% gold) and **B)** shell formation (80% gold). All scale bars are 100 nm.

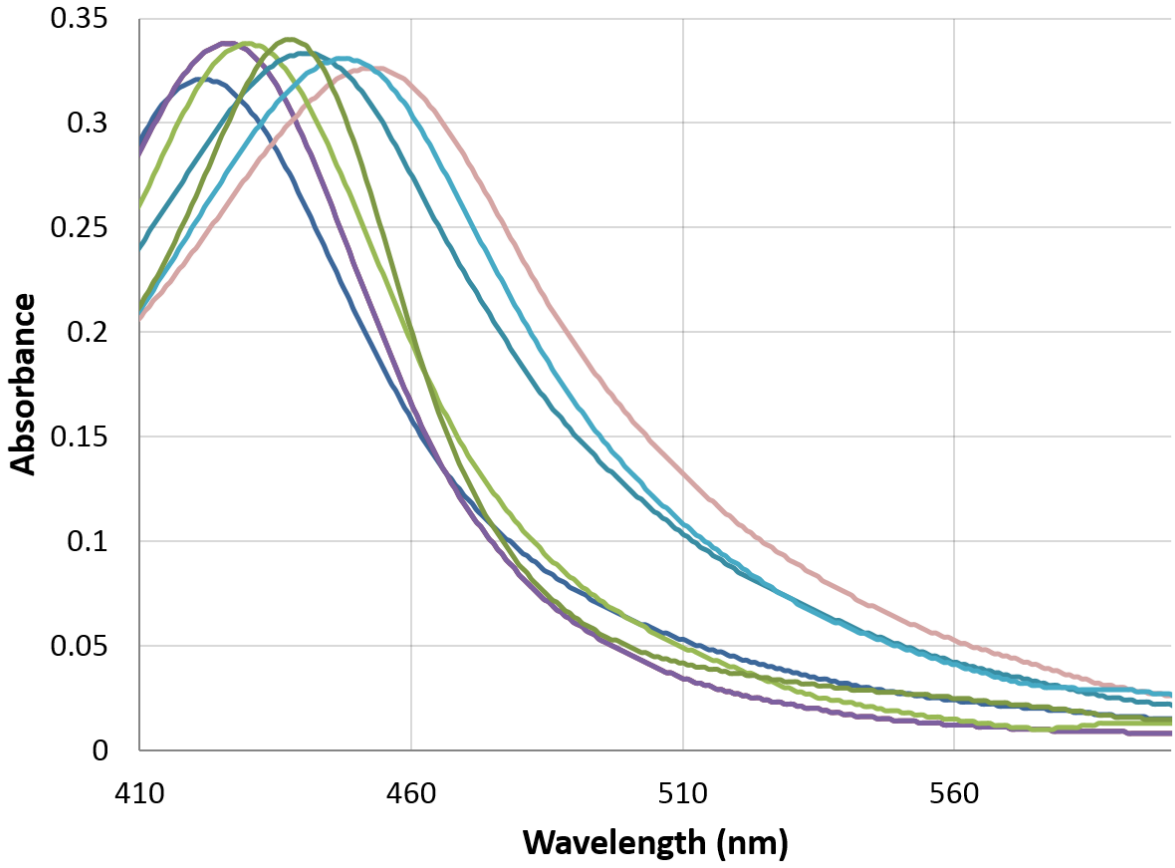

Figure S4. UV-vis spectra of prepared AgI_hNPs with the attainable range of SPR maxima from 420 to 455 nm.

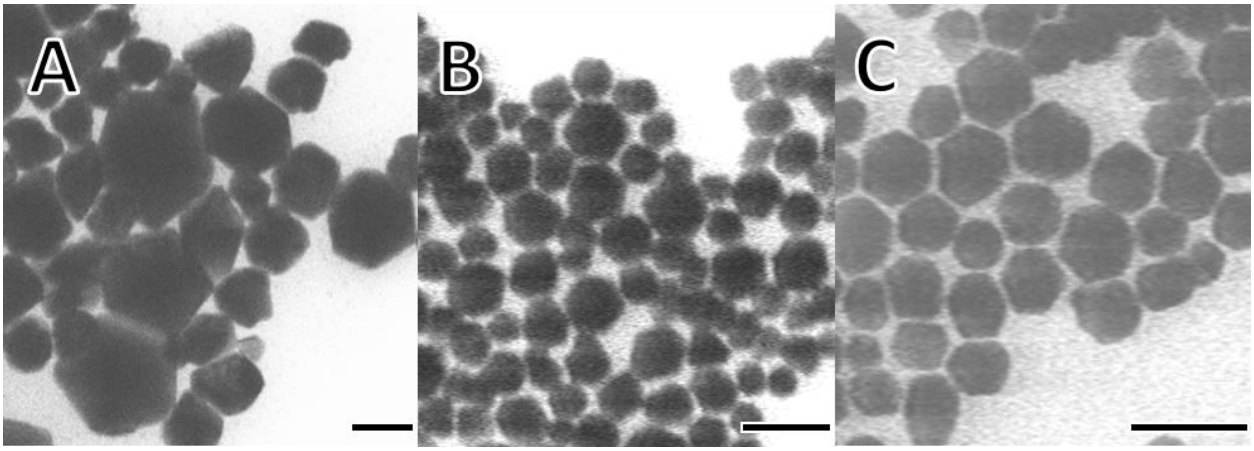

Figure S5. TEM images of AgI_hNP samples prepared: **A)** without copper; **B)** without hydrogen peroxide; **C)** using potassium persulfate instead of hydrogen peroxide. All scale bars are 100 nm.

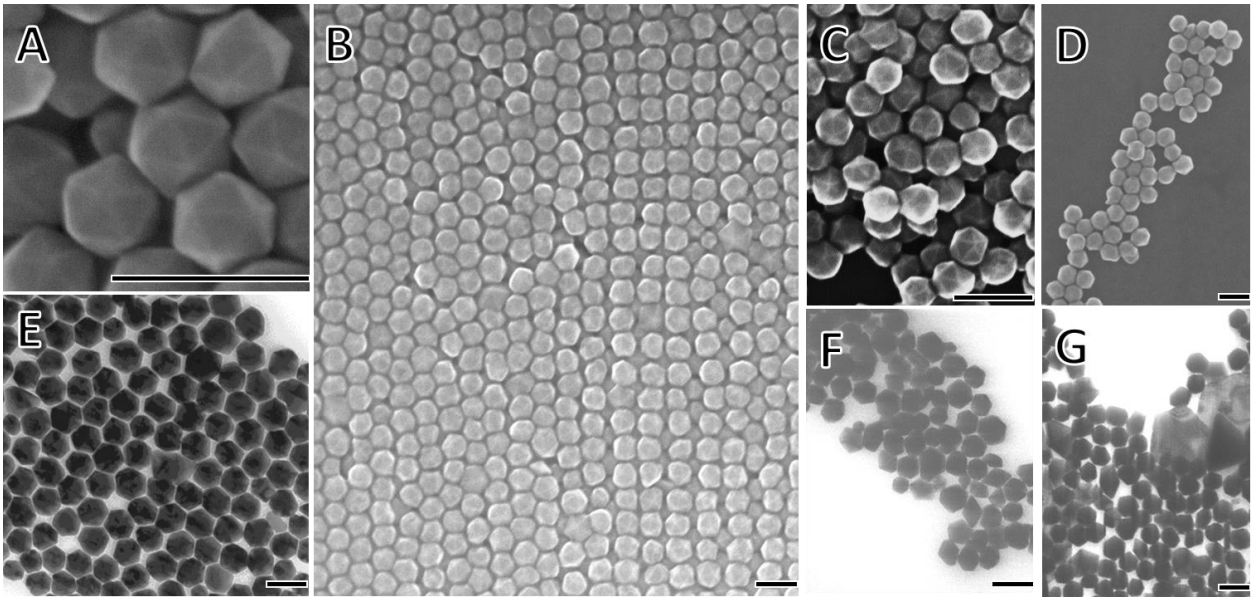

Figure S6. EM images demonstrating the effect of different sterically stabilizing polymers on size- and shape-selection in AgI_hNP synthesis: **A)** no polymer; **B)** 0.25 mM PVP; **C)** 0.016 mM PSS; **D)** 0.014 mM PSS; **E)** 0.026 mM PVP; **F)** 7.6 μM poly(vinylpyridine); **G)** 0.18 mM poly(acrylic acid). All scale bars are 100 nm.

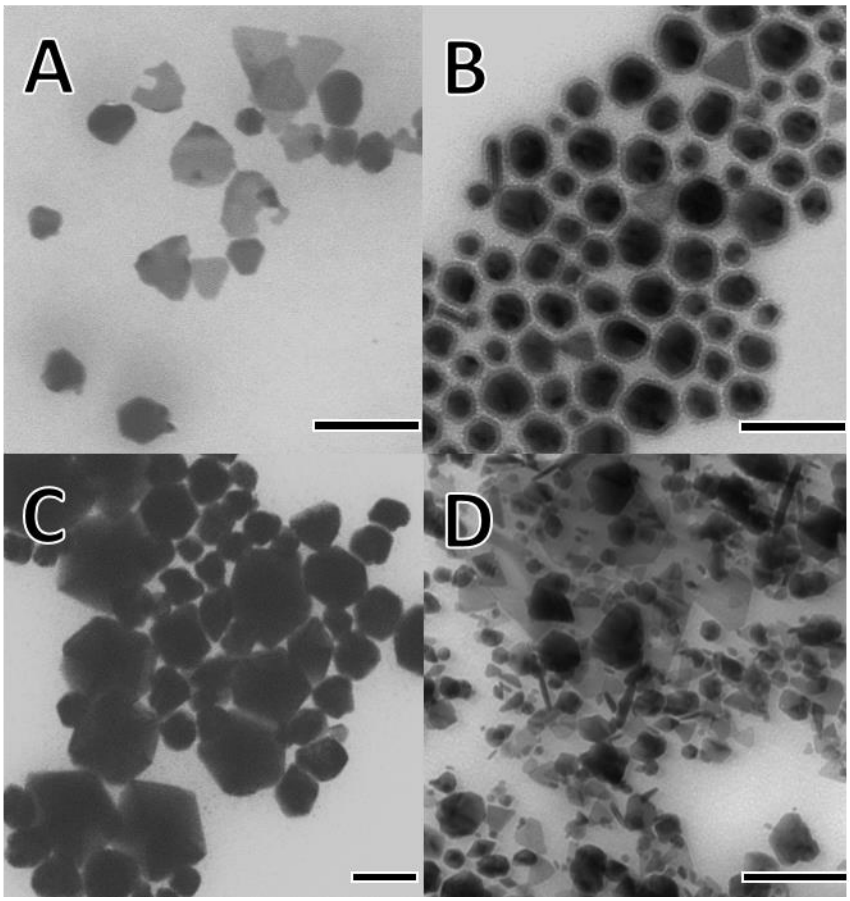

Figure S7. Transmission electron microscopy (TEM) images of AgI_hNPs prepared with and without metal dopants. **A)** Pd^{2+} (1:33 Pd/Ag molar ratio); **B)** Fe^{3+} (2.2:1 Fe/Ag molar ratio); **C)** No metal dopant; **D)** Co^{2+} (4.4:1 Co/Ag molar ratio). All scale bars are 100 nm.

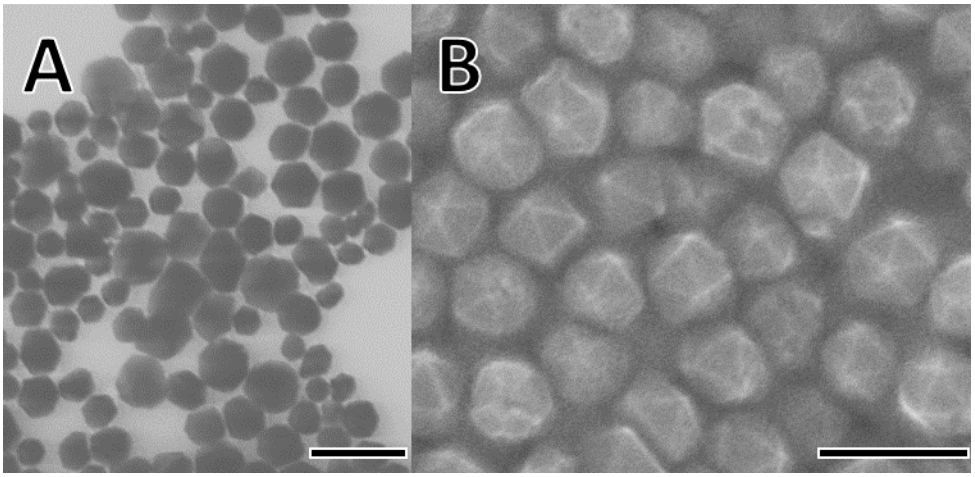

Figure S8. EM images of AgI_hNPs samples prepared with palladium or cobalt doping in addition to 0.29 mM copper. **A)** TEM of AgI_hNPs prepared with 2.02 µM Pd^{2+} and **B)** SEM of AgI_hNPs prepared with 1.82 µM Co^{2+}. All scale bars are 100 nm.

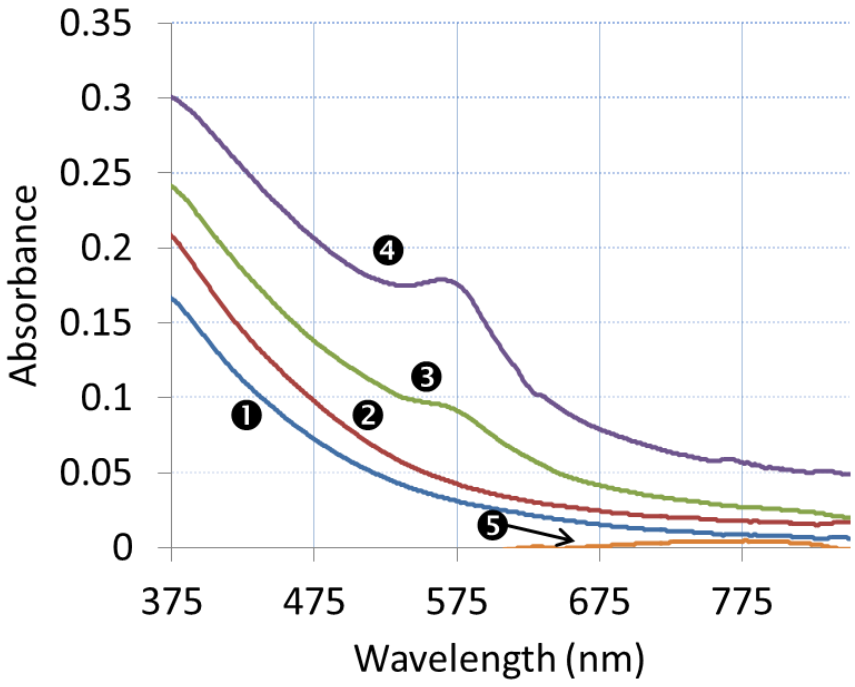

Figure S9. UV-vis spectra of AgI_hNP precursor mixture reduced without silver: copper sulfate (0.3 mM) reduction with sodium borohydride (2.95 mM) in the presence of sodium tricitrate (1.7 mM). ❶- immediately after reduction, ❷- 5 minutes after reduction, ❸- 15 minutes after reduction, ❹- 50 minutes after reduction, ❺- 4 hours after reduction.

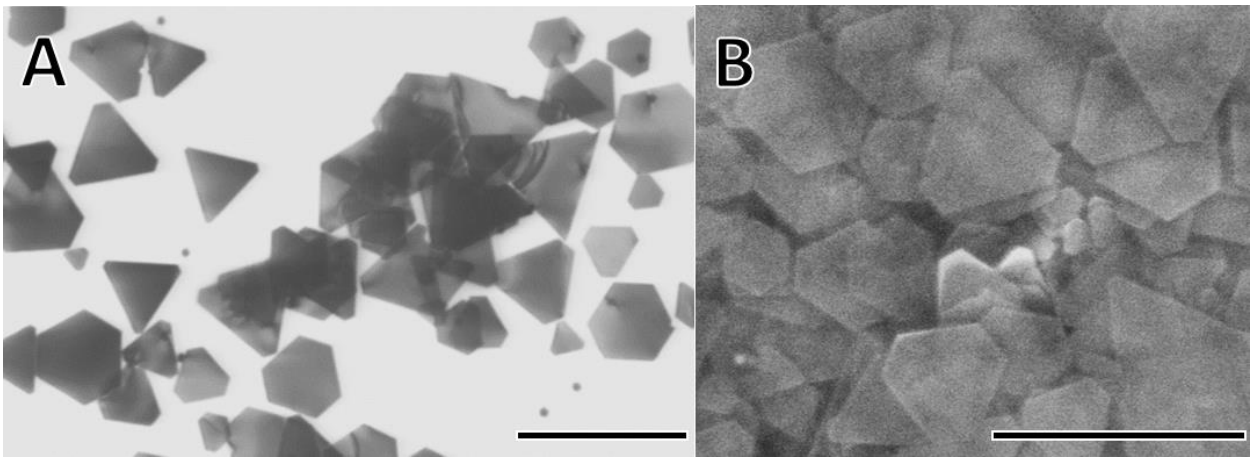

Figure S10. **A)** TEM and **B)** SEM images of silver platelets produced by thermal development of icosahedra precursor solution. All scale bars are 100 nm.

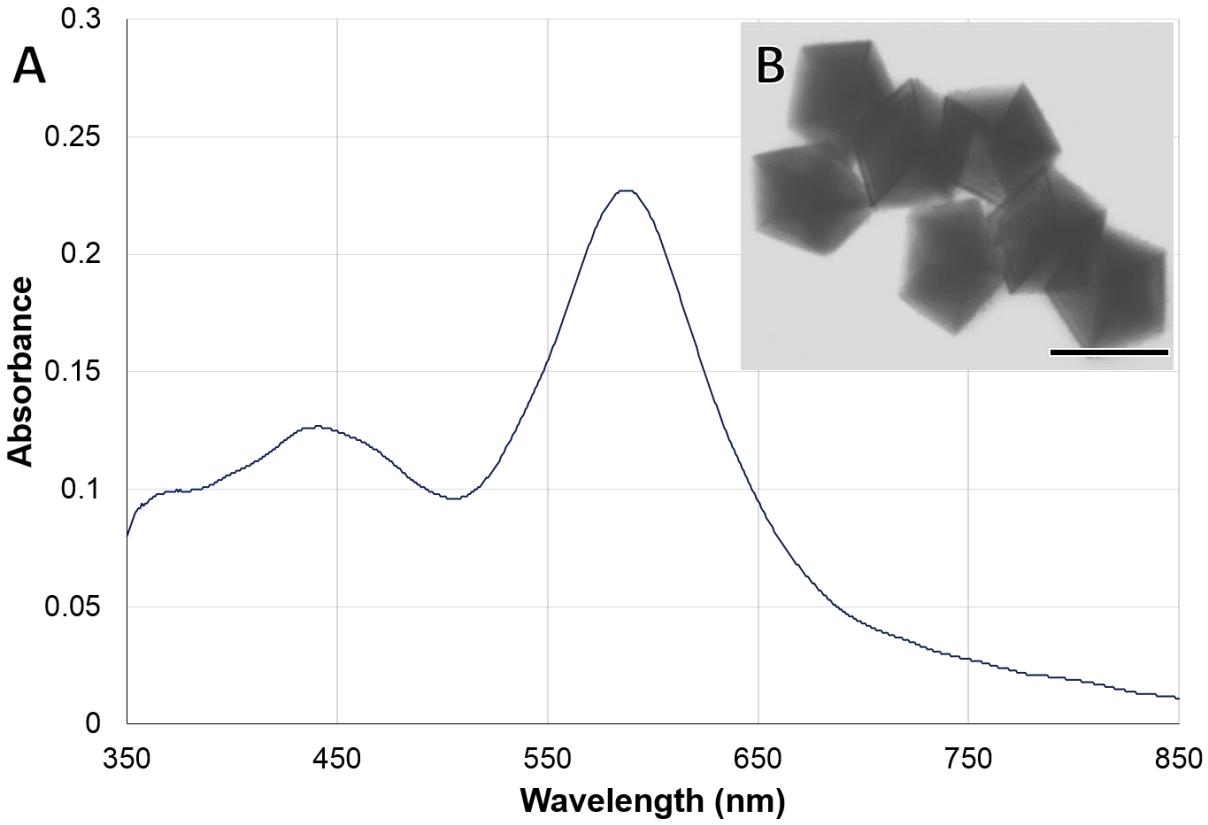

Figure S11. **A)** UV-vis spectrum and **B)** TEM image of decahedral AgNPs produced by exposure of precursor NPs to LED light of 435 nm emission wavelength. The scale bar is 100 nm.

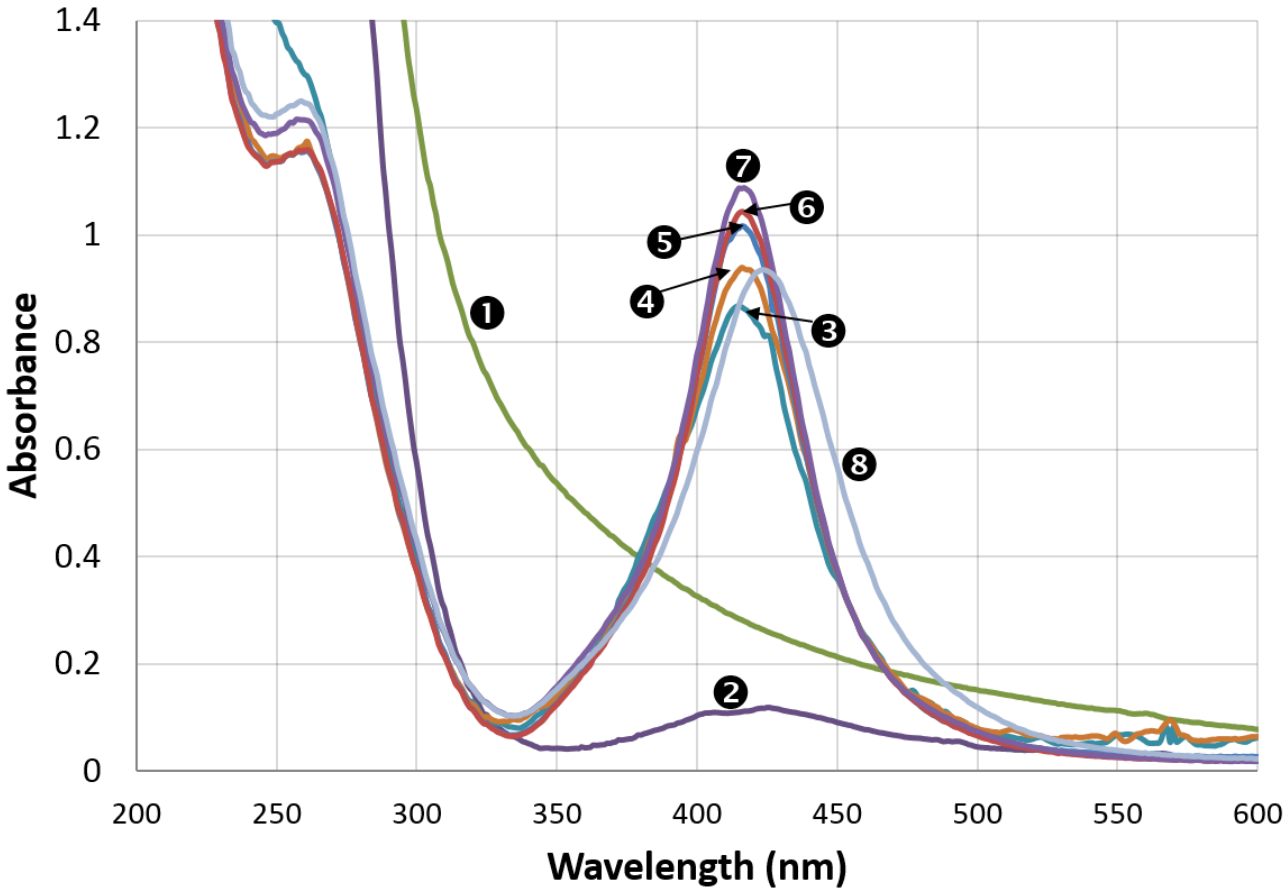

Figure S12. UV-vis spectra illustrating the time development of AgI_nNPs: ❶ immediately after H_2O_2 addition; ❷ 5 min of light exposure; ❸ 15 min; ❹ 30 min; ❺ 45 min ❻ 1 hr; ❼ 3.5 hrs; ❽ 19 hrs.

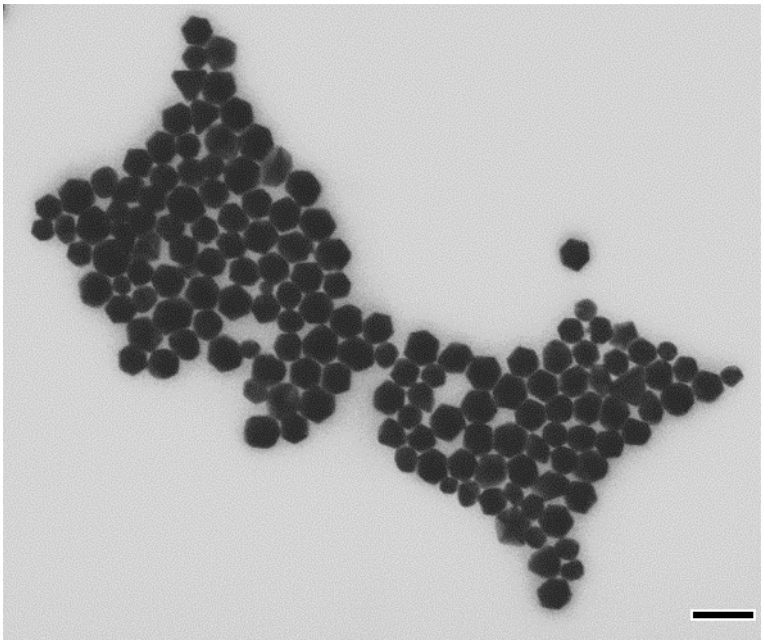

Figure S13. TEM image of AgI_hNP samples exposed to LED light for 1.5 hours. The scale bar is 100 nm.

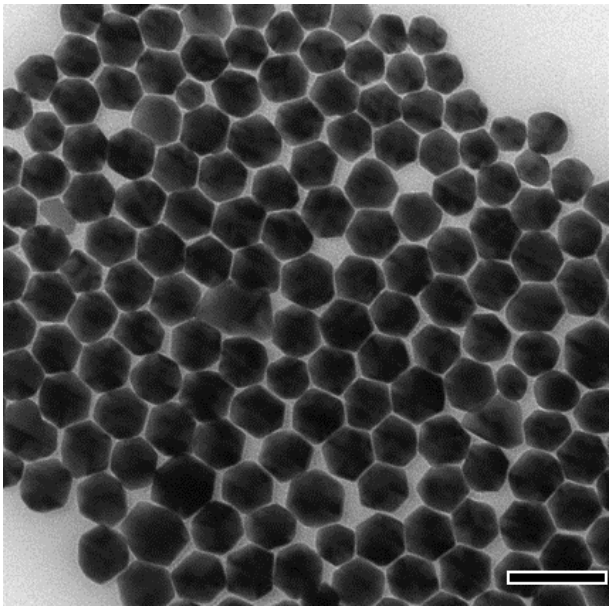

Figure S14. TEM image of AgI_hNPs subjected to thermal post-modification with KCl (7.4 μM). The scale bar is 100 nm.

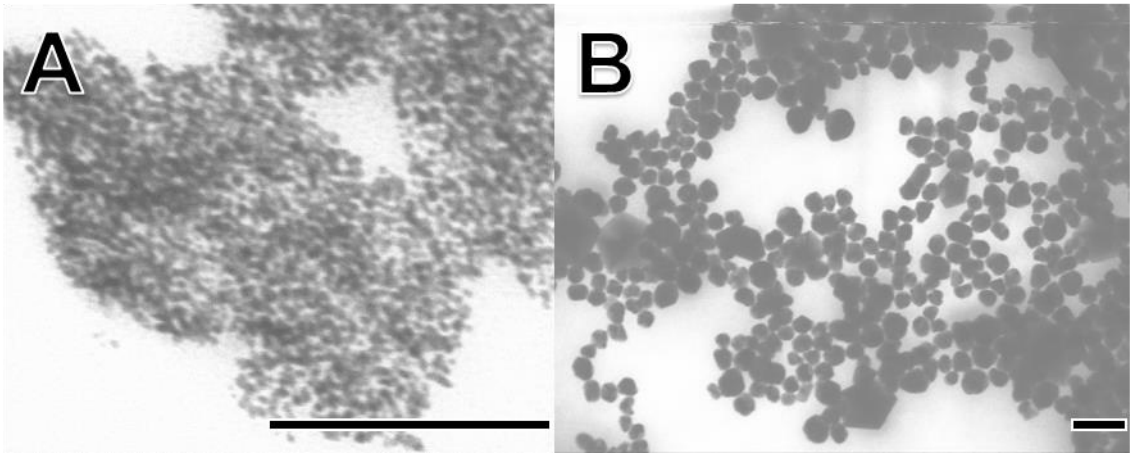

Figure S15. TEM images of the effect of addition of $[AuCl_4]^-$ to AgI_hNPs. **A)** AgI_hNPs prepared with gold (0.12 mM; 2:1 Au/Ag molar ratio) and copper (0.29 mM) and **B)** AgI_hNPs prepared without copper but with gold (5.4 µM; 1:12 Au/Ag molar ratio). All scale bars are 100 nm.

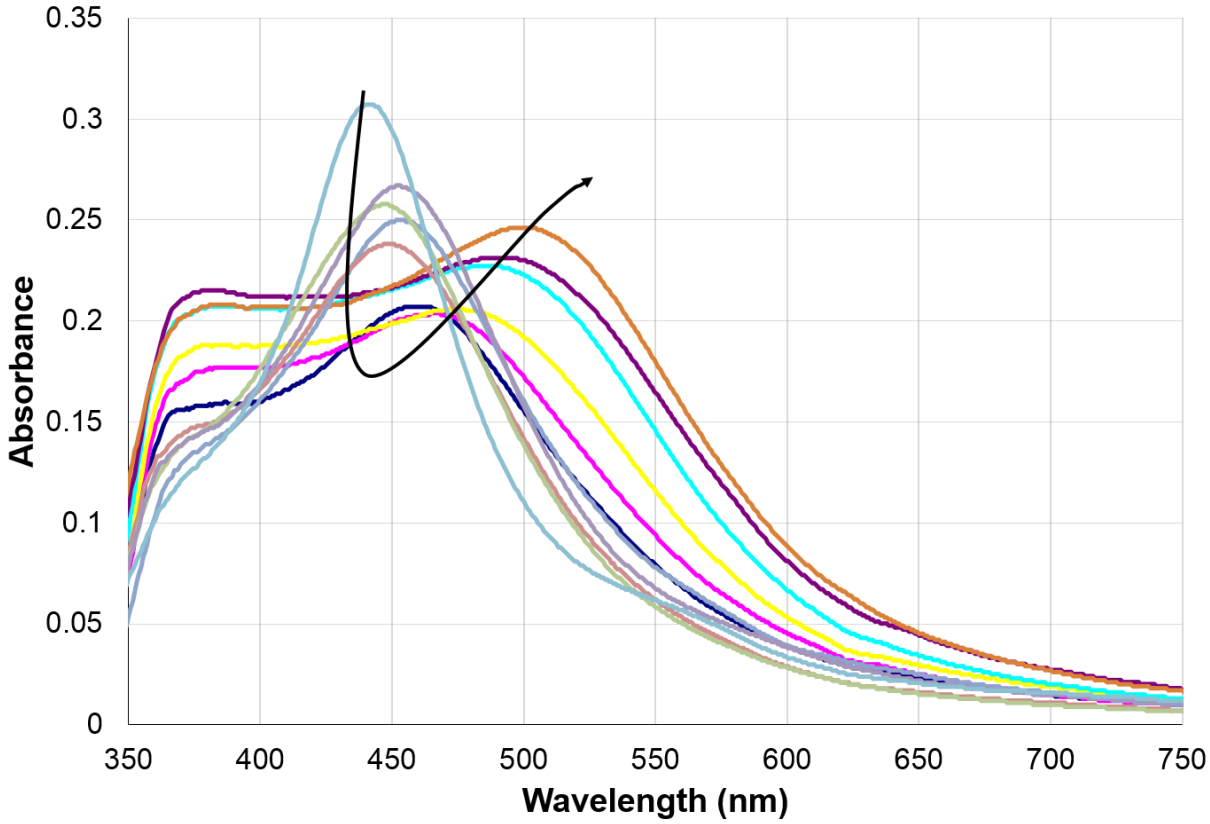

Figure S16. UV-vis spectra of the effect of gold doping in AgI_hNP synthesis. The arrow indicates progression of spectra with increasing gold concentration.

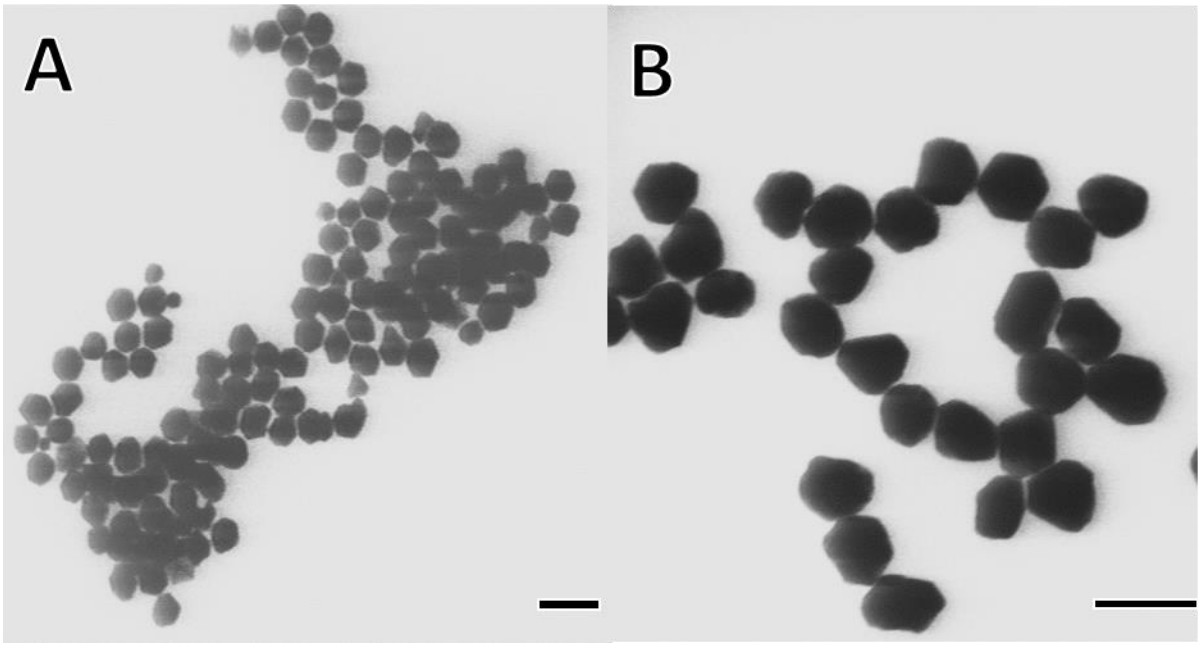

Figure S17. TEM images of AgI_hNPs prepared with **A)** 0.40 nM iodide and **B)** 22 nM bromide. All scale bars are 100 nm.

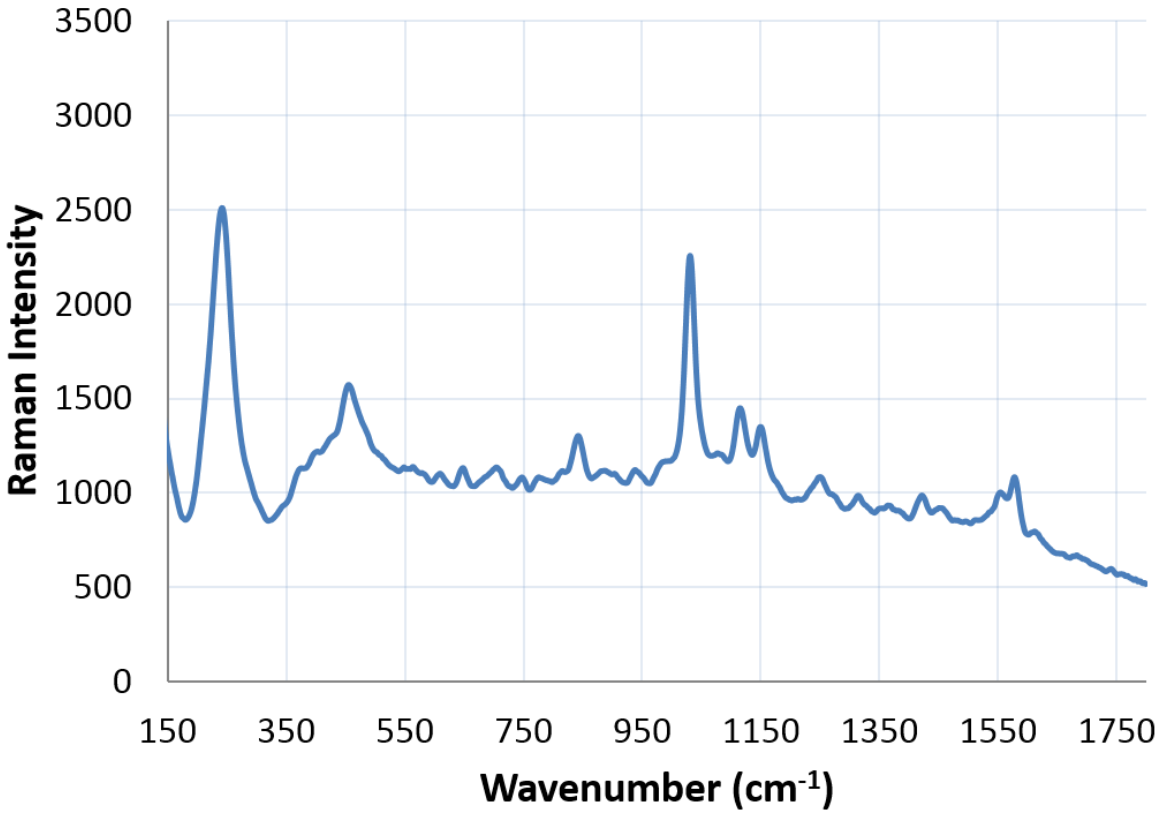

Figure S18. A representative SERS spectrum of 50 pmole of thiosalicylic acid recorded using a substrate of a dry film of AgI_hNPs with an average bilayer thickness.

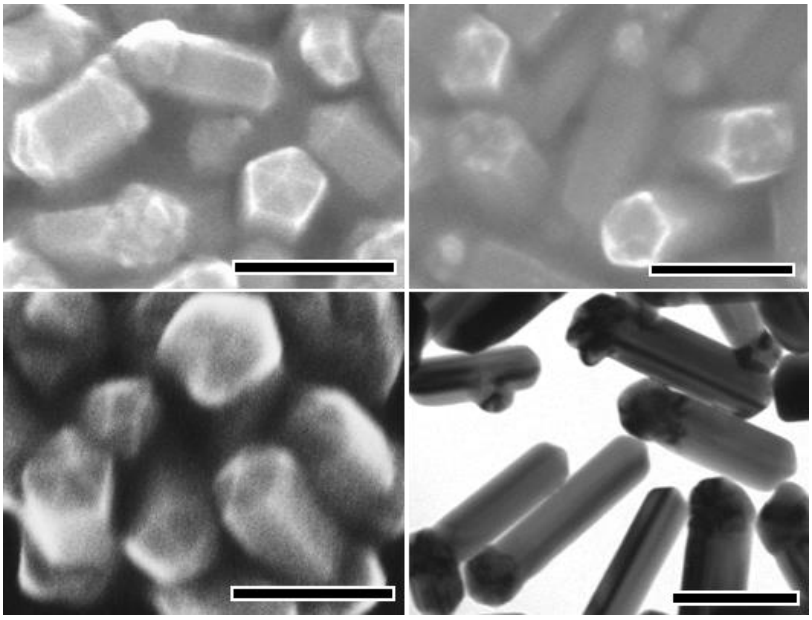

Figure S19. EM images demonstrating pentagonal cross-sections of pentagonal pins produced by 1-D thermal regrowth of AgI_hNPs. All scale bars are 100 nm.

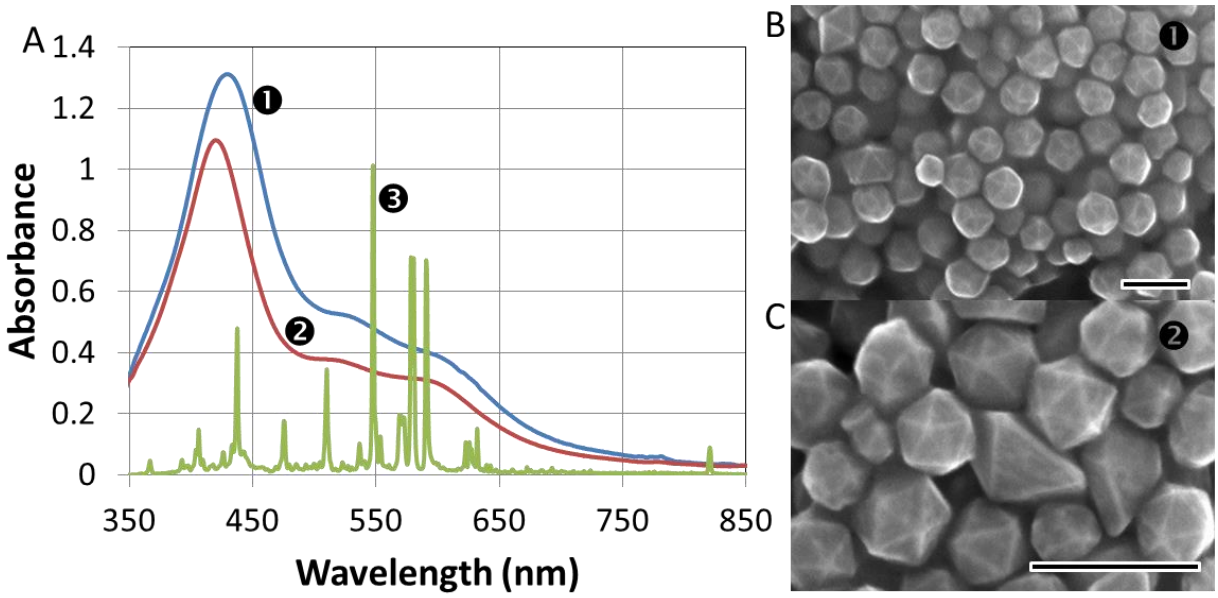

Figure S20. AgI_hNPs prepared using metal halide lamp exposure. **A)** UV-vis spectra of AgI_hNP samples (❶&❷) with overlaid spectrum of metal halide lamp (❸). **B)** and **C)** Corresponding SEM images of AgI_hNP samples ❶&❷. All scale bars are 100 nm.

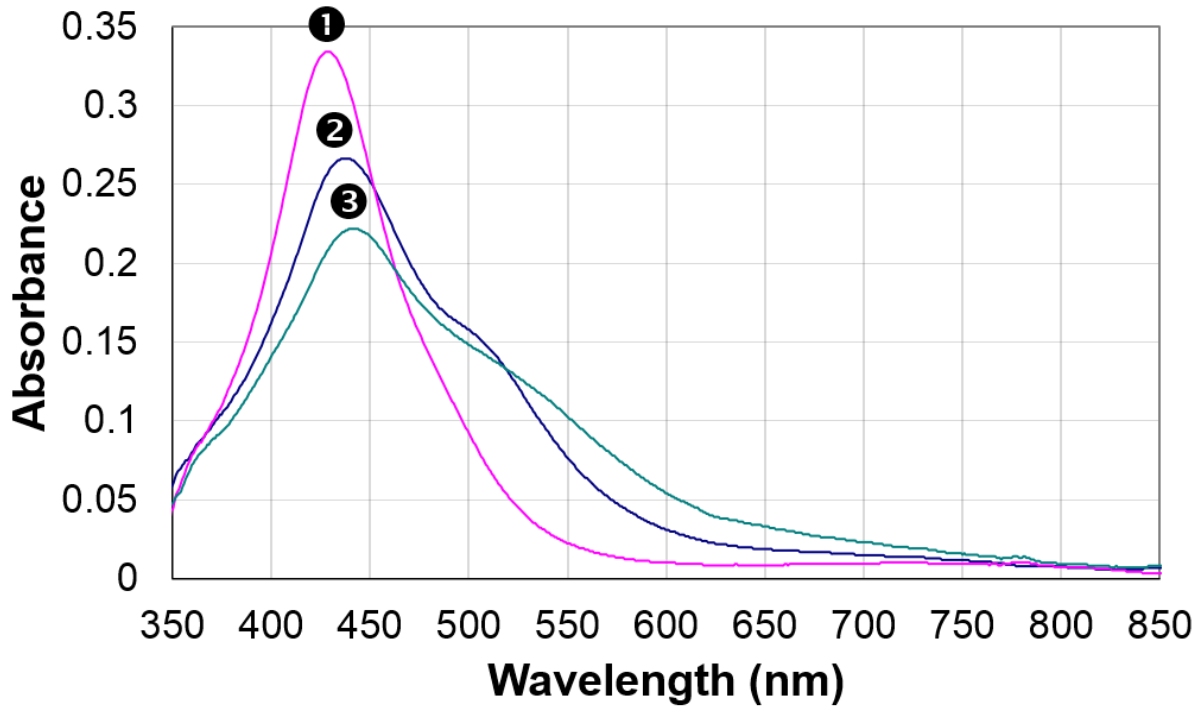

Figure S21. UV-vis spectra illustrating the effect of $NaBH_4$ concentration: total borohydride concentrations in the AgI_hNPs synthesis were ❶ 3.4 mM ❷ 2.2 mM ❸ 4.5 mM.

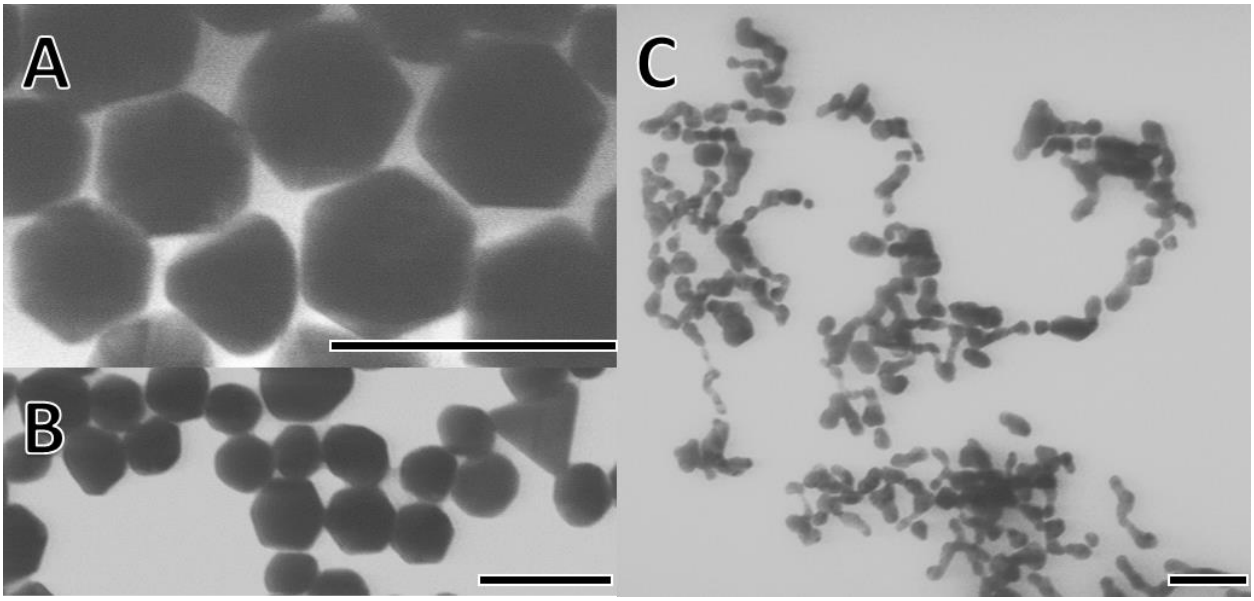

Figure S22. TEM images of samples prepared with ascorbate and citrate instead of sodium borohydride. **A)** 2.54 mM ascorbate with 7.05 µM PSS. **B)** 2.58 mM ascorbate without polymers. **C)** 67 µM citrate. All scale bars are 100 nm.

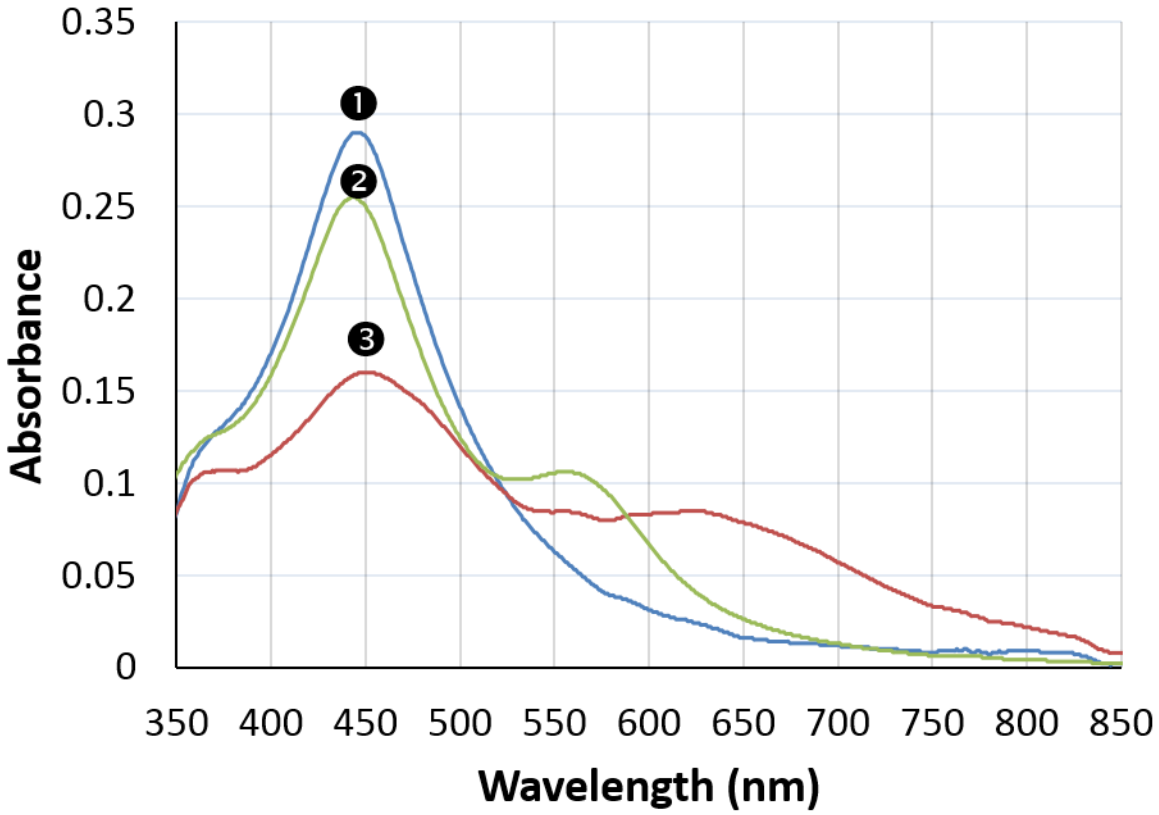

Figure S23. UV-vis spectra illustrating effects of tricitrate concentration: total tricitrate concentrations in the AgI_hNPs synthesis were ❶ 1.7 mM ❷ 1.8 mM ❸ 2.3 mM.

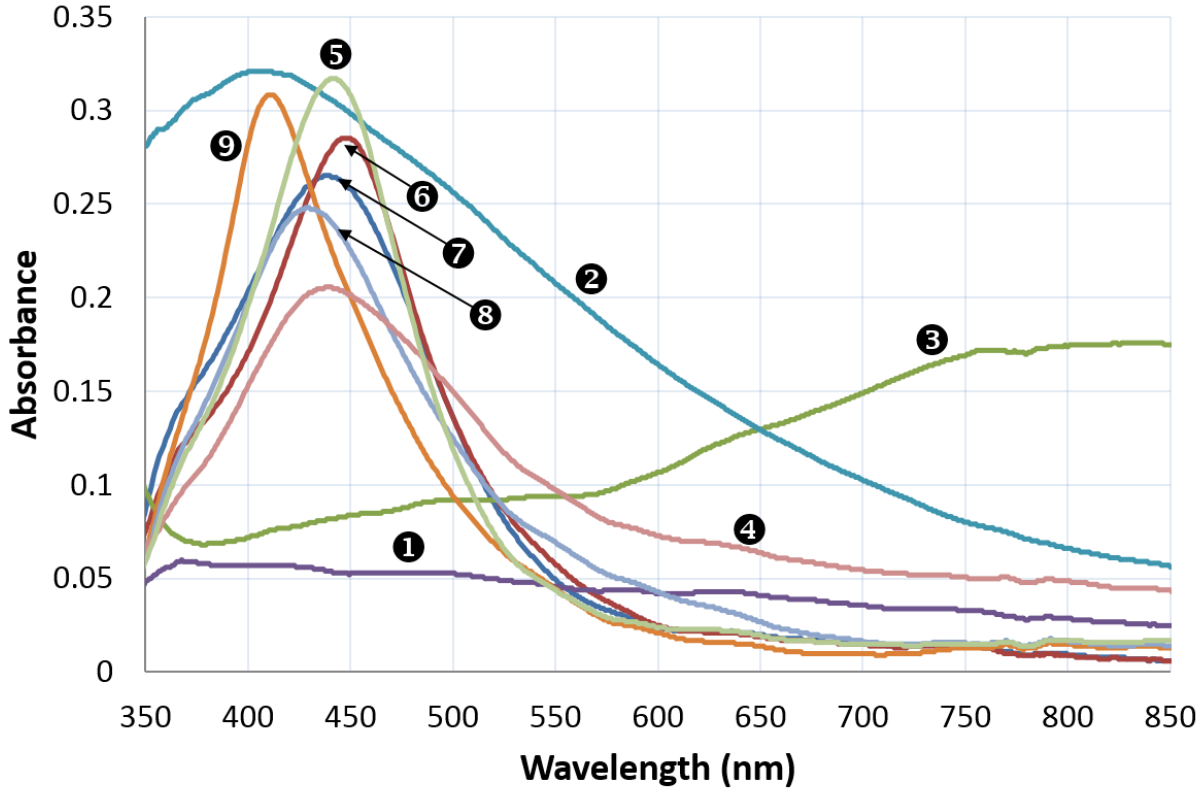

Figure S24. UV-vis spectra illustrating the effect of pH on AgI_hNP synthesis: ❶ pH 11.5; ❷ pH 11.0; ❸ pH 10.5; ❹ pH 9.4; ❺ pH 8.8; ❻ pH 8.2; ❼ pH 7.9; ❽ pH 7.0; ❾ pH 6.4.

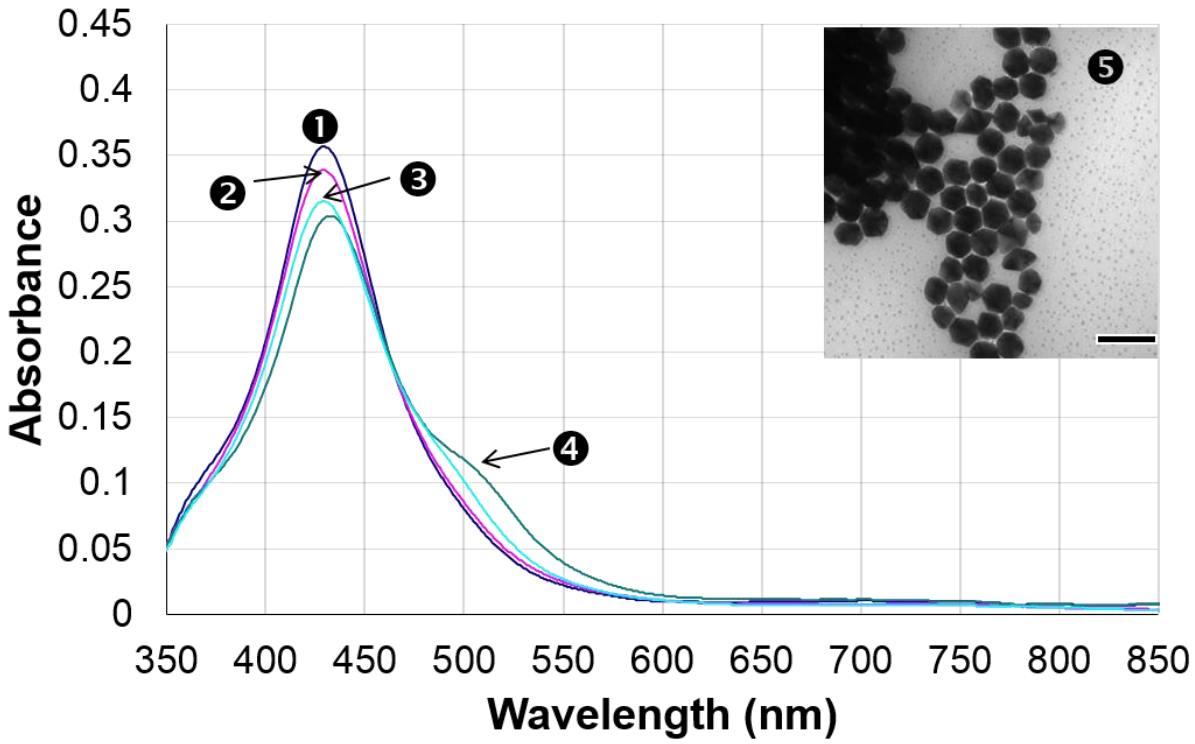

Figure S25. UV-vis spectra demonstrating the effect of the rate of stirring using a 12.7 mm x 3.2 mm cylindrical stir bar on AgI_hNP synthesis. ❶ No stirring, gently shaken between the additions of reagents; ❷ spinning at 90 rpm; ❸ spinning at 700 rpm; ❹ spinning at 250 rpm. Inset ❺ is TEM image of AgI_hNPs prepared without stirring, gently shaken between the additions of reagents (spectrum❶). The scale bar is 100 nm.

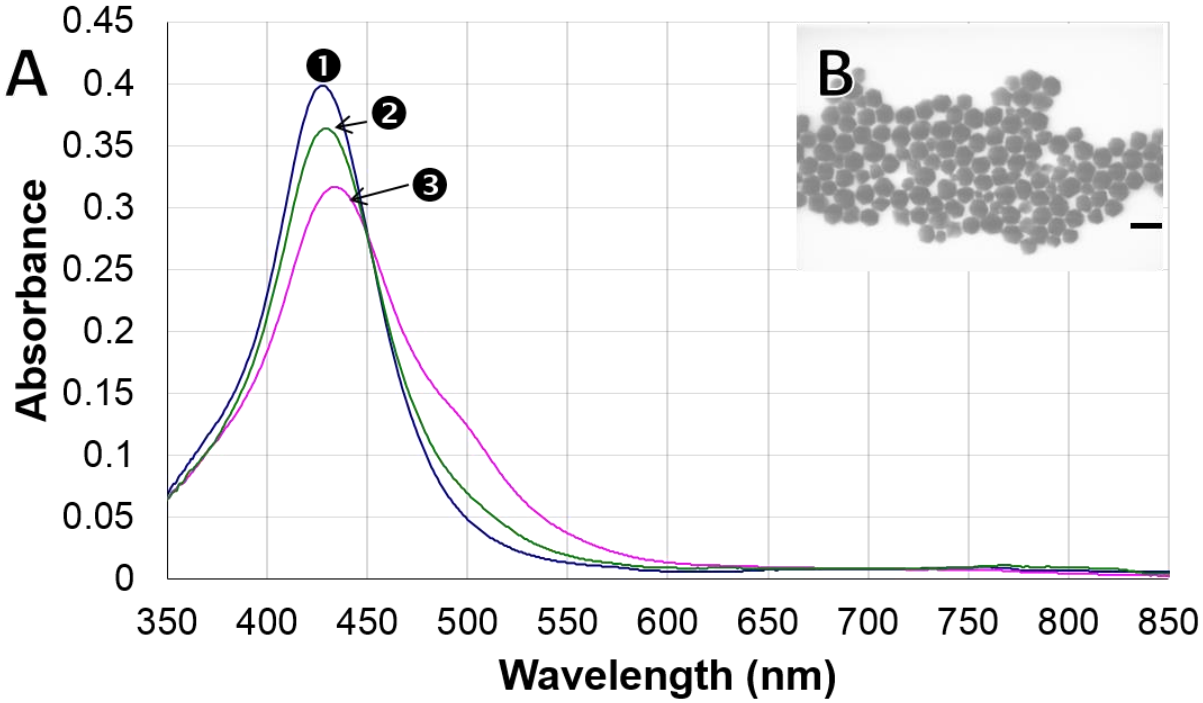

Figure S26. **A)** UV-vis spectra demonstrating the effect of different types of stir bars at 90 rpm stirring rate on the development of AgI_hNPs: ❶ 9.5 mm × 9.5 mm × 5.5 mm cross stir bar; ❷ 12.7 mm × 3.2 mm cylindrical stir bar; ❸ 15.9 mm × 9 mm large octagonal stir bar. **B)** TEM image of AgI_hNPs prepared using 9.5 mm cross stir bar. The scale bar is 100 nm.

References

[1] N. Murshid, D. Keogh, V. Kitaev, *Part. Part. Syst. Charact*. 2014, **31**, 178-189.

[2] K. G. Stamplecoskie, J. C. Scaiano, *J. Am. Chem. Soc.* 2010, **132**, 1825−1827.

[3] N. Cathcart, V. Kitaev, *ASC Nano* 2011**, 5**, 7411-7425

[4] G. S. Metraux, C. A. Mirkin, *Adv. Mater.* 2005, **17**, 412-415.

[5] C. L. Cleveland, U. Landman, *J. Chem. Phys*. 1991, **94**, 7376-7396.

[6] X. Wu, P. L. Redmond, H. Liu, Y. Chen, M. Steigerwald, L. Brus, *J. Am. Chem. Soc.* 2008, **130**, 9500-9506.

[7] N. Murshid, I. Gourevich, N. Coombs, V. Kitaev, *Chem. Commun*. 2013, **49**, 11355-11357.

[8] M. McEachran, D. Keogh, B. Pietrobon, N. Cathcart, I. Gourevich, N. Coombs, V. Kitaev, *J. Am. Chem. Soc.* 2011*,* **133***,* 8066-8069.